Published in final edited form as:
J Biomed Opt. 2009 ; 14(2): 024040. doi:10.1117/1.3120490.

Femtosecond laser ablation of the stapes

Ryan G. McCaughey,
University of California, Irvine, Beckman Laser Institute and Medical Clinic, 1002 Health Sciences Road, Irvine, Calfornia 92612

Hui Sun,
University of California, Irvine, Department of Ophthalmology, 118 Med Surge I, Irvine, Calfornia 92697

Vanessa S. Rothholtz,
University of California, Irvine, Department of Otolaryngology-Head and Neck Surgery, Irvine Medical Center, Building 56, 101 The City Drive South, Orange, Calfornia 92868

Tibor Juhasz, and
University of California, Irvine, Department of Ophthalmology, 118 Med Surge I, Irvine, Calfornia 92697

Brian J. F. Wong
University of California, Irving, Beckman Laser Institute and Medical Clinic, 1002 Health Sciences Road, Irvine, Calfornia 92612

Abstract

A femtosecond laser, normally used for LASIK eye surgery, is used to perforate cadaveric human stapes. The thermal side effects of bone ablation are measured with a thermocouple in an inner ear model and are found to be within acceptable limits for inner ear surgery. Stress and acoustic events, recorded with piezoelectric film and a microphone, respectively, are found to be negligible. Optical microscopy, scanning electron microscopy, and optical coherence tomography are used to confirm the precision of the ablation craters and lack of damage to the surrounding tissue. Ablation is compared to that from an Er:YAG laser, the current laser of choice for stapedotomy, and is found to be superior. Ultra-short-pulsed lasers offer a precise and efficient ablation of the stapes, with minimal thermal and negligible mechanical and acoustic damage. They are, therefore, ideal for stapedotomy operations.

Keywords

fermtosecond phenomena; lasers in medicine; electron microscopy; thermal effects

Address all correspondence to: Ryan G McCaughey, Beckman Laser Institute and Medical Clinic, University of Calfornia, Irvine, 1002 Health Sciences Road, Irvine, CA 92612. Tel: 949-824-0534; Fax: 949-824-8413; rmccaugh@uci.edu.

1 Introduction

Otosclerosis is the abnormal growth of bone in the otic capsule. It often results in fixation of the stapes footplate to the oval window, resulting in conductive hearing loss.[1] Treatment is usually by a stapedotomy—a perforation is created in the stapes footplate, into which a piston-like prosthetic device is inserted and coupled to the incus.[2] Surgical procedures of the stapes and middle ear require precision, while minimizing damage to sensitive inner ear structures and the facial nerve.

A high-power laser is commonly used to fenestrate the stapes. Numerous lasers have been used[3] for this procedure, including argon (518 nm), KTP Nd:YAG (532 nm), Er:YAG (2940 nm), and CO_2 (10600 nm). However, none of these lasers are ideal for performing stapedotomy. For example, the visible light of argon and KTP lasers is weakly absorbed by the perilymph, and therefore penetrates to the sensitive hearing and balance organs of the inner ear. The IR light of Er:YAG and CO_2 is more readily absorbed, but short high-energy pulses result in large pressure transients, which could cause acoustic trauma.

An ideal laser system for middle ear surgery would have thermal and stress confinement. Femtosecond (fs) laser pulse ablation occurs with minimal thermal or mechanical injury. Tightly focused high-intensity ultrashort pulses ionize material to produce a mixture of free electrons and ions, termed plasma, in the focal point of the laser beam. Laser energy is then absorbed by the plasma, so that the process is only weakly dependent on the tissue characteristics. Ablation is very precise because it is confined to the region of ionization. There is little or no heating outside the targeted area because ablation occurs more rapidly than thermal diffusion.[4] Ultrashort laser pulses have been shown to effectively ablate bone and hard tissue.[5–10] This study evaluates the ablation of ossicular bone with a femtosecond laser, commonly used in LASIK eye surgery.[11]

2 Materials and Methods

A Model I Intralase FS laser (AMO Corp, Santa Ana, California), commonly used for LASIK eye surgery, was used to irradiate the bone. The laser produces 1053-nm, 700-fs pulses of up 10 μJ with a repetition rate of 10 kHz. The diameter at the focal point of the laser beam in air is approximately 3 μm (as quoted by Intralase specifications). Computer-controlled mirrors scanned the beam in a spiral pattern of increasing diameter with an accuracy of 1 μm. The planar glass window of the delivery system was removed because vaporized bone collected on the lens and shielded the sample from the laser. The focusing optics were not modified, and it is assumed the optical properties of the beam were not significantly altered by removing the glass window. The focus of the laser beam was aligned with the surface of the sample by adjusting the height of the sample relative to the laser output. The focus was determined to be coincident with the surface at the point at which bright visible plasma was observed.

Porcine otic capsule bone was ablated to emulate the stapedotomy operation. The otic capsule surrounds the membranous labyrinth of the inner ear and provides a hard bony casing to protect the organs of hearing and balance. The stapes footplate is derived from the otic capsule, so they are histologically and embryologically similar.[12] The otic capsule was

removed from the temporal bones of fresh pig skulls, obtained from a large regional packing company (Clougherty Packing LLC, Los Angeles, California). The skulls were divided in a midsaggital plane. The brain was carefully removed to expose the otic capsule that lies along the middle section of the petrous ridge. The otic capsule in the domestic pig is separate from the rest of the temporal bone and is easily pried loose with a narrow osteotome. The entire otic capsule was removed intact and is approximately 2 × 2 × 3 cm in size. A low-speed microstructural saw with a 0.3-mm diamond wafering blade (Buehler, Lake Bluff, Illinois) was used to machine the bone into slices approximately 1 mm thick, to represent the stapes.

Temporal bones were obtained from cadavers through the Willed Body Program at the University of California, Irvine. Each specimen was examined for otosclerosis, other disease processes and erosion of the stapes. Access to the middle ear was acquired via a tympanomeatal flap. The incudostapedial joint was visualized and carefully dislocated. The stapedial tendon was sectioned, and the stapes was removed in its entirety, maintaining the integrity of the stapes superstructure and footplate.

Figure 1 shows a model vestibule, which grossly conforms to volumetric measurements from temporal bone atlases. It was constructed by drilling a 3-mm-diam hole through the center of an acrylic block. Three small ports (1 mm in diameter) were drilled from the side of the block into the cavity to enable the insertion of a thermocouple. The ports were positioned 1.0, 3.0, and 5.0 mm below the upper surface of the chamber. The chamber was filled with water to mimic perilymph. For further details see Ref. 13. A type E, beaded, 24AWG glass braid insulated wire thermocouple (Omega Co., Stamford, Connecticut) connected to an integrated signal conditioning data acquisition module (NI-USB 9211A, National Instruments, Austin, Texas) was used to measure the temperature in the model vestibule.

Photomechanical stress was measured with a piezoelectric fluoropolymer film (PVDF) transducer (SDT series, Measurement Specialties, Inc., Hampton, Virgenia) connected to a data acquisition module (NI-USB 6211, National Instruments, Austin, Texas). The piezo film produces voltage in proportion to compressive or tensile mechanical stress (piezo stress constant, $g_{33} = -330 \times 10^{-3}$ V m^{-1}/N m^{-2}). Ultrasound gel (Aquasonic 100, Parker Laboratories, Inc., Fairfield, New Jersey) was placed between the PVDF and the bone specimen to minimize acoustic reflections. Acoustic events were recorded with a unidirectional dynamic microphone (frequency response: 50 to 15,000 Hz, impedance: 600 Ω, sensitivity: −72±3 dB, RadioShack) 2 cm from the bone sample.

Optical coherence tomography (OCT) of the ablation craters was carried out with a Niris Imaging System (Imalux Corporation, Cleveland, Ohio). It has a lateral resolution of ≤50 μm and a depth resolution of 10 to 20 μm.

Microscopy was performed with a Philips XL30 Scanning Electron Microscope (FEI, Hillsboro, Oregon). Samples were fixed in osmium tetraoxide, dehydrated, and sputter coated with gold prior to imaging with the scanning electron microscope (SEM).

3 Results

3.1 Porcine Otic Capsule

Irradiation of the otic capsule slices resulted in a bright plasma on the surface of the bone. The threshold for a visible plasma was 0.6 μJ (approximately 8.5 J/cm^2). A scan spiral of 3 mm diameter took 78 s, while 1 mm took 20 s. The time to complete the scan increased quadratically with scan diameter.

Figure 2 shows ablation from a femtosecond beam of 10-μJ pulse energy with a separation of 3 μm between each scan position, scanned over an area 3 mm in diameter. It is compared to ablation by 10 0.15-J pulses from an Ultrafine Er:YAG laser (Coherent Inc, Santa Clara, California). Measurement by OCT found the crater from the femtosecond laser to be 90±10 μm deep. No evidence of thermal damage or charring was observed when ablating with the femtosecond laser. The crater base and walls of the femtosecond ablation are considerably smoother and better defined than those created by Er:YAG, as shown in Fig. 2. The OCT images [Figs. 2(b) and 2(f)] show that the femtosecond laser produces perpendicular crater walls and a flat base, compared to the ErYAG crater that has sloping walls and a base that is deeper at the periphery than in the center.

The SEM images of the femtosecond crater edge [Fig. 2(c)] confirm that the ablated area ends abruptly, with no damage to the surrounding bone. In comparison, the Er:YAG crater [Fig. 2(g)] has no clear boundary—a region of approximately 100 μm of damaged tissue encircles the crater. Figures 2(d) and 2(h) show the base of the femtosecond and Er:YAG craters, respectively. The rings of the scanned femtosecond beam are evident in Fig. 2(d). The surface is much smoother than the Er:YAG base [Fig. 2(h)].

Figure 3 shows the temperature increase on the back surface of a 1-mm slice of otic capsule for spiral patterns of different diameters. Every 10th data point was sampled for clarity. The thermocouple was in direct contact with the bone in the center of the spiral. The beam diameter was 3 μm with 1-μm separation between consecutive delivery positions. The energy per pulse was 10 μJ. The temperature growth and decay follow the same trend, but the maximum temperature increase is greater for larger spiral diameters.

Figure 4 shows the temperature increase on the rear surface of a 1.35-mm thick otic capsule slice for pulse energies 10, 8, 6, 4, 2, and 1 μJ in a 0.5-mm scan diameter. The beam diameter was 3 μm, with a separation of 1 μm. The maximum temperature increase is linear with respect to pulse energy, as shown in Fig. 5.

Figure 6 shows how the temperature increase in the model ear 1 mm below the stapes for a 10-μJ pulse scanned over 0.5 mm. The temperature increase 3 and 5 mm below the stapes in the model ear was negligible.

Any photoacoustic stress or sound was too small or out of the range of the detectors to record. By comparison a 300-μs, 50-J/cm^2 pulse (parameters used for efficient ablation) from an Er:YAG laser generates[14] a peak stress of 43 kPa.

3.2 Human Stapes

Figure 7 shows a human stapes with a 0.5-mm-diam perforation in the footplate created with the femtosecond laser. A 10-μJ beam focused to 3 μm ablated the 70-μm footplate. The SEM image confirms that the perforation is a smooth cut with well-defined edges.

4 Discussion

The findings of precise ablation of otic capsule bone were duplicated in the human stapes. The well-defined ablation crater and the lack of damage to surrounding tissue created by the femtosecond laser will ensure a potentially smoother fit for prosthetic devices used in stapedotomy. The small beam size coupled with computerized scanning of the femtosecond device means precise perforations of any shape can be obtained.

The temperature increases of the order of 1 °C associated with 10-μJ beams are well tolerated in middle ear surgery. Noyes et al. found that a temperature increase of 3 °C did not impair hair cell function in the rabbit cochlea.[15] Repetition of the procedure to achieve the desired ablation depth may be required, but this will result in only a modest accumulation of heat. The heat generated will not be easily transported to the sensitive inner ear organs, as evidenced by Fig. 6. One millimeter into the “perilymph,” the temperature increase is less than 0.1°C, and there is no noticeable temperature increase 3 mm beyond the stapes.

During ultra-short-pulse laser ablation, electrons are transferred to the conduction band of dielectric materials by multiphoton ionization and other nonlinear effects. Relaxation occurs through electron-phonon coupling (generation of heat) or by radiative decay (fluorescence). The absorbed energy is transferred to breaking of the material bonds, formation of excited fragments, and expulsion of the resulting vapors. A small part of the laser energy is transferred to the bulk through convective heating of the emerging plasma plume, electron-phonon relaxation without defragmentation and reabsorption of fluorescent radiation. This remaining energy heats the surrounding tissue. By observing the thermal effects in the irradiated tissue it is possible to estimate the proportion of the laser energy that contributes to heating the material.

The temperature from a time-dependent point source, at distances much greater than the size of the beam, can be approximated by

$$T = \int_0^t \frac{2\alpha Q}{8(\pi\tau)^{3/2} k(\chi)^{1/2}} \exp\left(-\frac{r^2}{4\chi\tau}\right) \mathrm{d}\tau, \quad (1)$$

where α is the fraction of the laser energy that contributes to heating, Q is the heat source, k is the conductivity, χ is the diffusivity, and r is the distance from the source.[13] The spiral scanning pattern has been simplified to a ring of increasing radius x such that $x \propto \sqrt{t}$. Solving Eq. (1) and fitting to the experimentally measured temperature, α was found to be 0.05. This is in good agreement with Neev et al. who found α to be 0.07 for dentin irradiated with a femtosecond laser.[16] Figure 8 compares the temperature increase measured on the

rear surface of a 1.35-mm-thick bone slice irradiated with 6-μJ laser pulses scanned over a 0.5-mm radius, and the temperature predicted by Eq. (1).

This model also predicts a linear increase in temperature with pulse energy, in agreement with the measured trend shown in Fig. 5.

The thermoelastic expansion of the high-energy density plasma and the recoil stress from the ejection of ablated material should generate mechanical stresses. However, no pressure wave or acoustic events were measured during ablation. This may be because the short time periods involved result in shock waves of very high frequency (~gigahertz). Such high frequencies do not propagate well in tissue, and the energy is reabsorbed within a few micrometers.[17] This observation is in agreement with results obtained with optical measurements indicating the short (10- to 20-μm) decay of shockwaves generated with femtosecond photodisruption in water and in corneal tissue.[18] Neev et al. also reported negligible acoustic events when ablating hard tissue with an ultra-short-pulse laser.[19] This offers femtosecond ablation a significant advantage over Er:YAG, which is characterized by a loud popping. This is especially important for middle ear surgery where acoustic events could cause trauma to sensitive inner ear organs.

Future studies will include *in vitro* measurements of temperature in human bone and *in vivo* studies of femtosecond laser use within the middle ear of animals and humans. A system is currently being developed to deliver this novel use of the femtosecond laser to the human temporal bone.

5 Conclusion

A femtosecond laser, normally used for LASIK eye surgery, was used to ablate porcine otic capsule bone and human stapes bones. Optical microscopy, OCT, and scanning electron microscopy show the ablation craters to be smooth and precise. Thermal side effects were shown to be minimal, and acoustic and mechanical events were negligible. These characteristics indicate that the Intralase FS device could have applications in middle ear surgery, including human stapedotomy.

Acknowledgments

The authors would like to thank Lih-Huei Liaw, MS, for her assistance with the microscopy.

References

1. Schuknecht, HF. Pathology of the Ear. Harvard University Press; Cambridge, MA: 1974.
2. Fisch U. Stapedotomy versus stapedectomy. Am J Otol. 1982; 4(2):112–117. [PubMed: 7148999]
3. Frenz M. Physical characteristics of various lasers used in stapes surgery. Adv Oto-Rhino-Laryngol. 2007; 65:237–249.
4. Vogel A, Venugopalan V. Mechanisms of pulsed laser ablation of biological tissues. Chem Rev (Washington, DC). 2003; 103(2):577–644.
5. Girard B, Yu D, Armstrong MR, Wilson BC, Clokie CML, Miller RJD. Effects of femtosecond laser irradiation on osseous tissues. Lasers Surg Med. 2007; 39(3):273–285. [PubMed: 17311312]

6. Armstrong WB, Neev JA, Da Silva LB, Rubenchik AM, Stuart BC. Ultrashort pulse laser ossicular ablation and stapedotomy in cadaveric bone. Lasers Surg Med. 2002; 30(3):216–220. [PubMed: 11891741]
7. Neev J, Nelson JS, Critelli M, McCullough JL, Cheung E, Carrasco WA, Rubenchik AM, Silva LBD, Perry MD, Stuart BC. Ablation of human nail by pulsed lasers. Lasers Surg Med. 1997; 21(2):186–192. [PubMed: 9261796]
8. Schwab B, Hagner D, Bornemann J, Heermann R. The use of femtosecond technology in Otosurgery. Femtosecond Technology for Technical and Medical Applications. 2004:211–226.
9. Liu Y, Niemz M. Ablation of femural bone with femtosecond laser pulses—a feasibility study. Lasers Med Sci. 2007; 22(3):171–174. [PubMed: 17242869]
10. Ilgner J, Wehner M, Lorenzen J, Bovi M, Westhofen M. Morphological effects of nanosecond- and femtosecond-pulsed laser ablation on human middle ear ossicles. J Biomed Opt. 2006; 11(1): 014004. [PubMed: 16526881]
11. Binder PS. Flap dimensions created with the IntraLase FS laser. J Cataract Refractive Surg. 2004; 30(1):26–32.
12. Wong B, Liaw LH, Neev J, Berns M. Scanning electron microscopy of otic capsule and calvarial bone ablated by a holmium-YAG laser. Lasers Med Sci. 1994; 9(4):249–260.
13. Wong BJF, Lee JP, Dickinson MR, Neev J, Svaasand LO. Photothermal-induced temperature changes in a model inner ear: A comparison of visible, infrared, and ultraviolet lasers. IEEE J Sel Top Quantum Electron. 1996; 2(4):951–958.
14. McCaughey RG, Wong BJF, Tafoya J, Sun Y, Jain R. Compact infrared laser for stapedotomy. Proc SPIE. 2008; 6842:68421E.
15. Noyes WS, McCaffrey TV, Fabry DA, Robinette MS, Suman VJ. Effect of temperature elevation on rabbit cochlear function as measured by distortion-product otoacoustic emissions. Otolaryngol-Head Neck Surg. 1996; 115(6):548–552. [PubMed: 8969760]
16. Neev J, Da Silva LB, Feit MD, Perry MD, Rubenchik AM, Stuart BC. Ultrashort pulse lasers for hard tissue ablation. IEEE J Sel Top Quantum Electron. 1996; 2(4):790–800.
17. Oraevsky AA, Da Silva LB, Rubenchik AM, Feit MD, Glinsky ME, Perry MD, Mammini BM, Small WI, Stuart BC. Plasma mediated ablation of biological tissues with nanosecond-to-femtosecond laser pulses: relative role of linear and nonlinear absorption. IEEE J Sel Top Quantum Electron. 1996; 2(4):801–809.
18. Juhasz T, Kastis GA, Suárez C, Bor Z, Bron WE. Time-resolved observations of shock waves and cavitation bubbles generated by femtosecond laser pulses in corneal tissue and water. Lasers Surg Med. 1996; 19(1):23–31. [PubMed: 8836993]
19. Neev J, Huynh DS, Carrasco WA, Wilder-Smith PBB, Da Silva LB, Feit MD, Perry MD, Rubenchik AM, Stuart BC. Thermal and noise level characteristics of hard dental tissue ablation with 350-fs pulse laser. Proc SPIE. 1996; 2672:262–271.

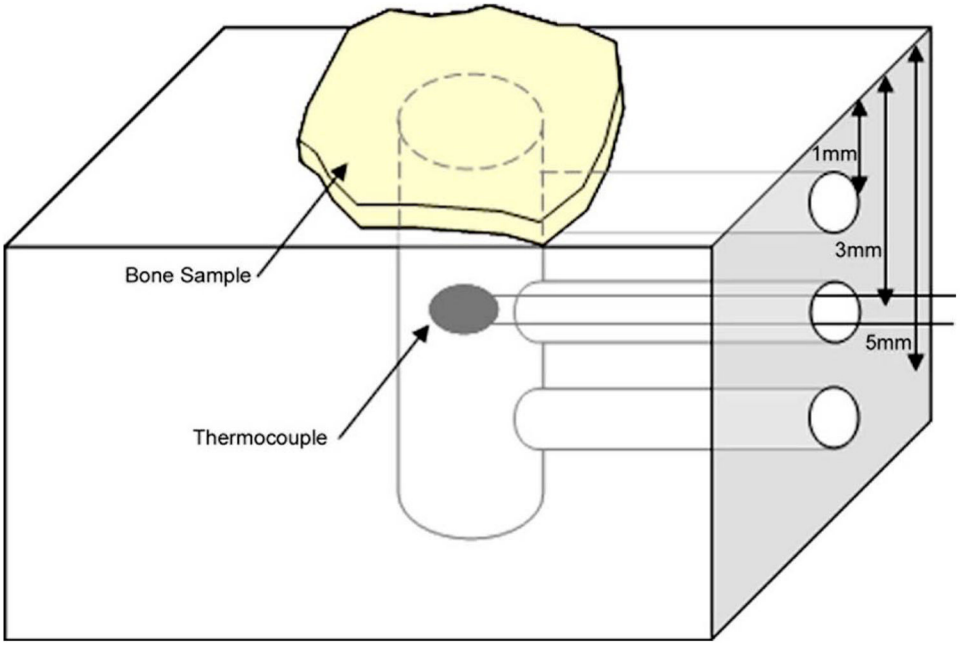

Fig. 1.
Schematic of model inner ear for measuring temperature during ablation of the stapes.

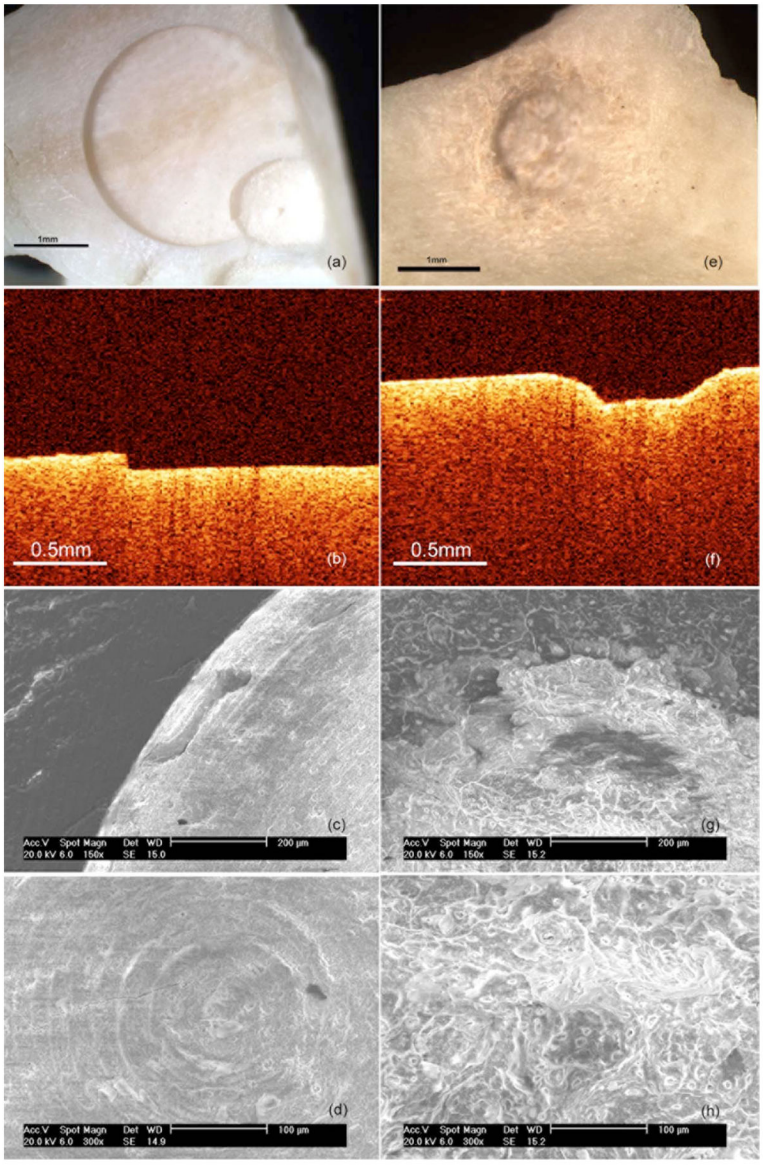

Fig. 2.

Otic capsule bone ablated with femtosecond (a) to (d) and Er:YAG (e) to (h) lasers: (a) and (e), light microscopy; (b) and (f), OCT; (c) and (g), SEM×150; and (d) and (h), SEM×300.

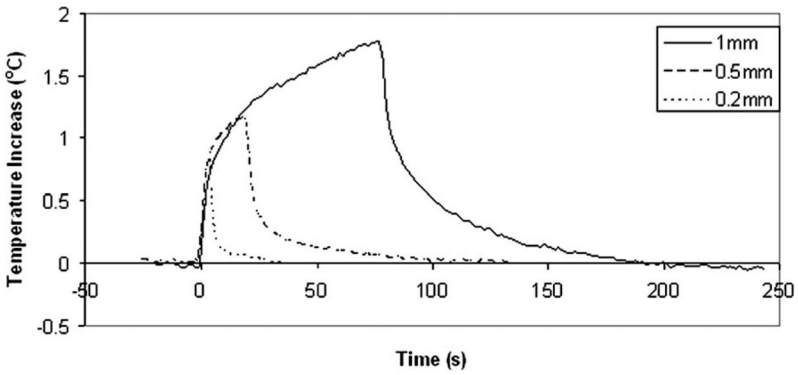

Fig. 3.

Temperature increase on the back surface of a 1-mm slice of otic capsule for spiral patterns of different diameters.

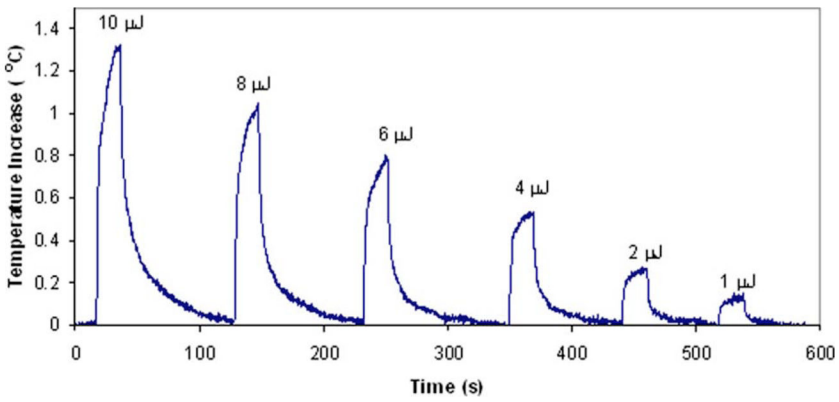

Fig. 4.

Temperature increase on the rear surface of a 1.35-mm otic capsule slice for different pulse energies.

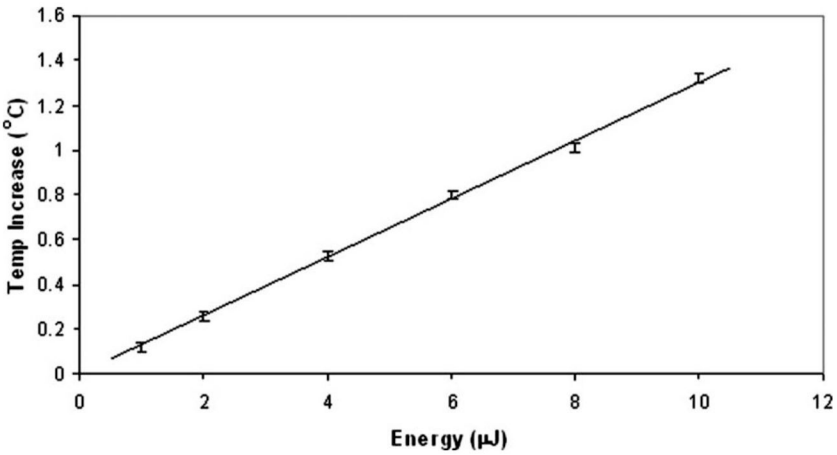

Fig. 5.
Maximum temperature increase as a function of energy.

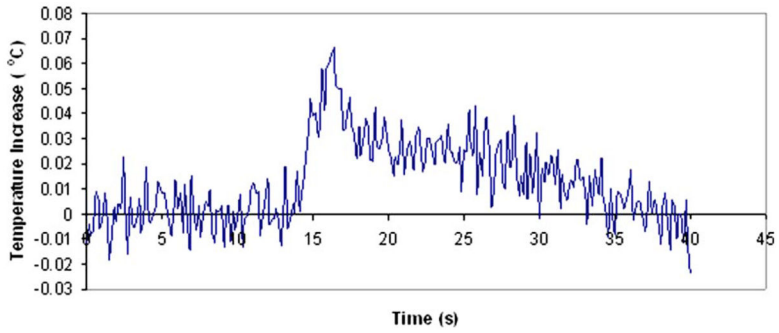

Fig. 6.

Temperature increase in model ear 1 mm below the stapes for a 10-μJ pulse scanned over 0.5 mm.

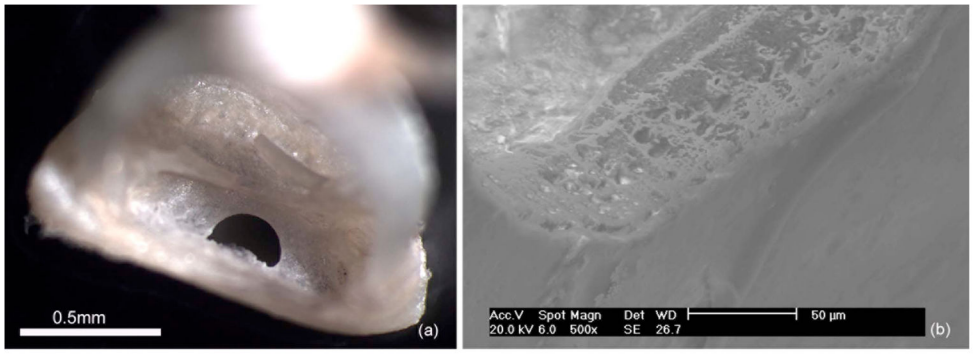

Fig. 7.

Human stapes footplate ablated by a femtosecond laser: (a) light microscopy of whole stapes and (b) SEM×500 of the perforation wall.

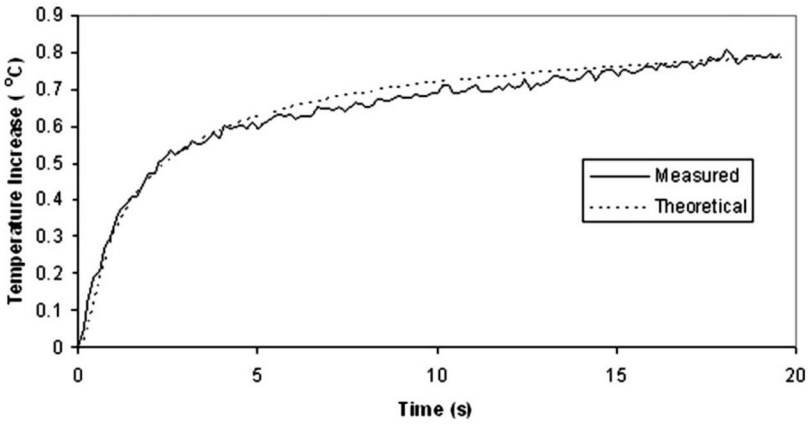

Fig. 8.

Comparison of the temperature increase measured on the rear surface of a 1.35-mm-thick bone slice irradiated with 6-μJ laser pulses scanned over a 0.5-mm radius, and the temperature predicted by Eq. (1).